X-ray reflection spectroscopy of the HfO2/SiO2/Si system in the region of the O-K absorption edge

E. O. Filatova, Philippe Jonnard, Jean-Michel André

X-ray reflection spectroscopy of the HfO$_2$/SiO$_2$/Si system in the region of the O-K absorption edge

E. O. Filatova

Institute of Physics, St. Petersburg State University, Ulyanovskaya 1, St. Petersburg, Petrodvorets 198904, RUSSIA

P. Jonnard, J.-M. André

Laboratoire de Chimie Physique-Matière et Rayonnement, Université Pierre et Marie Curie, CNRS UMR 7614, 11 rue Pierre et Marie Curie, 75231 Paris Cédex 05, FRANCE

Abstract

The x-ray reflection spectra, i.e. the reflected intensity as a function of the incident photon energy, of the HfO$_2$/SiO$_2$/Si system in the region of the O-K absorption edge are observed for various glancing angles. It is demonstrated that the variation of the glancing angle enables the depth profilometry of the sample. By using the Kramers-Kronig analysis, the reflection spectra are transformed into absorption spectra, from which the local physico-chemical environment of the oxygen atoms can be deduced. Thus we show in a non-destructuve way that the HfO$_2$ amorphous film has a well defined structure with a thin superficial layer presenting defect points or various local atomic structures.

I. Introduction

Scaling down below 0.1 μm complementary-metal-oxide-semiconductor devices requires traditional SiO_2 gate dielectric thickness smaller than 2 nm [1]. This results in unacceptable leakage current arising from direct tunneling of electrons through the layer. The use of a physically thicker layer of an alternative "high-k" dielectric material may address leakage and reliability issues. Increases in the relative permittivity compared to SiO_2 (ε_k=3.9) [2,3] permit to use physically thicker films to obtain the same effective capacitance as devices with physically thinner SiO_2 layers, thereby providing the potential for many orders of magnitude reductions in direct tunneling current.

HfO_2 is one of the most attractive "high-k" dielectric material due to its high permittivity (ε_k=16-45) [4,5], high resistivity and high thermal stability. Many efforts have been invested in the study of the $HfO_2/SiO_2/Si$ system. The bulk of the experimental information comes from photoelectron spectra [6-16], which provide detailed information on the electronic structure of the material. Fewer experimental works on the conduction-band structure have been reported [17-21].

This work reports on the applicability of x-ray reflection spectroscopy for characterization of $HfO_2/SiO_2/Si$ system. The reflection spectrum exhibits "edges" due to the elements present in the specimen. Moreover the reflection near-edge structure is very sensitive to the sort of absorbing atoms, to their chemical state and to their local coordination environment [22,23].

The main objective of this study is to demonstrate the interest of the soft x-ray reflection spectroscopy as a nondestructive in-depth characterization tool of the local atomic structure of "high k" dielectric planar systems. For sake of clarity, the current discussion includes the reflection spectra in SiO_2/Si system measured for different incidence angles.

II. Experimental approach

The $HfO_2/SiO_2/Si$ sample is prepared with the following process [16]. The silicon substrate is first cleaned in a solution of HF 1%-diluted in deionized water. Then, the surface is slowly reoxidized in a controllable way, using a solution containing HCl and H_2O_2. This way, a 0.3 nm-thick SiO_2 layer is formed, as checked by ellipsometry. The 5 nm-thick HfO_2 layer is deposited by ALD (atomic layer deposition), using $HfCl_4$ and H_2O as precursors. Transmission electron microscopy (TEM) experiment has shown that the HfO_2 layer is amorphous [16].

A sample with a 120-nm thick SiO_2 layer on a top of a Si substrate is prepared. The Si substrate is a silicon single-crystal of p-type. The film is prepared by a dry oxidation method at about $1050°C$. In this case, the surface of the sample is formed in the process of spontaneous growth of dioxide on the crystalline silicon substrate.

The measurements are performed with synchrotron light sources. In any case, the spectral resolution is better than 0.1 eV around the O-K edge.

III. Results and discussion

Figures 1 and 2 display the reflection spectra of the $HfO_2/SiO_2/Si$ and SiO_2/Si systems measured in the vicinity of the K-edge of oxygen for different glancing angles. Analysis of the absolute reflectivity points out that the reflectivity for the smallest angle 2° is low in the $HfO_2/SiO_2/Si$ system ($\approx25\%$) in comparison with the SiO_2/Si system ($\approx75\%$). The increase of the glancing angle (that means an increase of the depth probing) reduces less the reflectivity for the $HfO_2/SiO_2/Si$ system than for the SiO_2/Si system. For example, the reflectivity is about 5% in the $HfO_2/SiO_2/Si$ system compared to about 1% in the SiO_2/Si system at 6°.

What is the most significant is the manifestation of the interfacial boundary in the reflection spectra in both systems. While the Kiessig fringes are visible in the SiO_2/Si system even at 4° (the structure around 531 eV in Fig. 2), this structure ispractically invisible in the reflection spectra of the $HfO_2/SiO_2/Si$ system. One can find the pronounced Kiessig fringes only in the spectrum measured for the largest glancing angle, at 30° around 530 eV(Fig. 1b).

One can see (Fig. 1a) that the reflectivity in the $HfO_2/SiO_2/Si$ obtained for the angle 6° is larger at all energies than the reflectivity measured for the angle 5°. Such phenomenon is possible only in the case where the material with other optical characteristics or an interlayer is involved in the process of formation of the reflected beam. Consequently, one can suggest that the depth of the formation of the reflected beam is larger than 100 nm for the 4° incidence angle in SiO_2 and is no larger then 5 nm in HfO_2 for the same angle. The obtained result is a good illustration of the concept of physically thick and thin films.

We try to compare the above results with the theoretical predictions of the formation depth of the reflected beam in both systems. This is done by taking into account that in the region of normal dispersion (far from the absorption edge) the atoms in condensed systems can be considered as independent scattering dipoles. This allows us to use the optical data from Henke and al. [24]. Figure 3 shows the angular dependencies of the reflection coefficient

calculated in the framework of Fresnel approach for 520 eV and 540 eV (before and after the O-K absorption edges) in the HfO_2 (density 9.68 g/cm^3) and SiO_2 (density 2.53 g/cm^3). It is necessary to remind that in the strict sense there is no critical angle of the total external reflection in the soft x-ray region due to the strong absorption of the materials. It is usual to speak about the range of angles where the reflectivity exists in this region. One can see (Fig. 3) that the reflectivity in the HfO_2 monotonously decreases with the angle and depends only slightly on the energy. There is not even a hint of the region of the total external reflection in HfO_2, but at the same time the noticeable reflection exists in wide angular region (0° - 8°). By contrast the shape of the reflectivity curves in SiO_2 depends strongly on the energy. Particularly striking is the quick fall of the reflectivity with the angle (0° - 5°) at both energies. Considering an exponential decrease in intensity, we have the following evaluation of the thickness of the layers determining the reflection in the x-ray region, or the radiation penetration depth:

$$1/D = 2 \, \omega/c \, Im(\varepsilon - \cos^2\theta_0)^{1/2} \qquad (1)$$

where D is the distance along the normal to the surface, θ_0 is the glancing angle, ε is the permittivity, ω is the angular frequency of the radiation and c is the light velocity.

According to our experimental and theoretical investigations [22] of the Si/SiO$_2$ system with different thicknesses of oxide, the equation (1) can be used to roughly estimate the formation depth of the reflected beam in materials within the region of normal dispersion. Figure 4 shows the calculated angular dependencies of the radiation penetration depth for different incident photon energies in HfO_2. The penetration depth in HfO_2 depends slightly on the energy and increases slowly with the increase of the angle. One can see for incident angles 4.5°-5°, that the layers determining the reflection in the vicinity of O-K edge is approximately 5 nm thick at all energies. This value agrees pretty well with our experimental result.

Now let us turn back to Fig. 1 and focus on the shape of the spectra and the energy positions of the main features of the fine structure. The spectra measured for 5°, 6° and 7° have a similar shape and only the energy shift caused by interferential effect in the direction of small energies takes place. The spectra obtained for small angles differ considerably.

Figure 5 presents the variation of the imaginary part of the dielectric function with the incident photon energy, which we call hereafter "absorption spectra", in the vicinity of the K edge of oxygen in the system HfO$_2$/SiO$_2$/Si calculated from the reflection spectra (Fig.1), by means of Kramers–Kronig relationships using the method described in Ref. [25]. The spectra

are normalized to the intensity of the first maximum. It should be emphasized that the calculated spectra agree well with the HfO_2 spectra obtained by x-ray absorption spectroscopy (XAS) and electron energy loss spectroscopy (EELS) of Refs. [17-21] describing the unoccupied density of states around the oxygen atoms.

Let us now consider the spectra step-by-step bearing in mind that the growth of the incident angle leads to an increase of the probing depth in the material. For convenience the absorption spectrum calculated from the reflection spectra for $\theta°$ will be symbolized by $\mu(\theta°)$. The spectrum $\mu(2°)$ is characterized by the lowest contrast. The significant increase of the absorption jump at 532 eV takes place in the spectrum $\mu(3°)$. Another significant change happens in the region of the peak b where a broad maximum with a slightly marked double structure appears. The increase of the angle, $\mu(4°)$, leads to a minor growth of the absorption jump but the most important evolution is: i) the change in the shape of the peak b as compared with $\mu(3°)$ and ii) the shift of the maximum of the peak b by 0.86 eV towards the low photon energy side in comparison with $\mu(2°)$. The energy position of the band a is conserved in all the discussed spectra.

As showed earlier, the formation of the reflected beam for 2°, 3° and 4° occurs inside the HfO_2 film but different thicknesses of the layer contribute to the reflection at each angle. Our results suggest that the investigated film is inhomogeneous in depth. The most plausible explanation for the marked changes can be given from the structural change point of view. The investigations [6,26] show that structural stability of the HfO_2 film is closely dependent on the thickness of the film. The unannealed HfO_2 films are amorphous when their thickness is below 8-10 nm. A TEM micrography of our 5 nm-thick sample confirms that the HfO_2 film is amorphous [16].

The correlation of the calculated spectra with the local coordination environment is now addressed. In the case of O-K absorption edge, the excitation of an electron from an oxygen atom 1s core level is considered. According to dipole selection rule the O-K edge reflects the local p-projected unoccupied density states of the conduction band. Moreover, because of the local character of the core hole, the structures observed near an absorption edge reflect the nearest neighbor coordination of the absorbing atom.

In Ref. [17,18] the *ab initio* results are presented for relatively small clusters that include the Hf atom at the center with eight O-atom neighbors. According to these

calculations, the anti-bonding O2p^* states are hybridized with the anti-bonding Hf 5d^* and Hf 6s^* states. The O 2p states in the HfO$_2$ reflect mainly the tail of the d states of the neighboring Hf atoms that make the lowest conduction band. Due to the effect of the crystal field from the oxygen atoms on the Hf d states, the fivefold-degenerated ^2D-term of the free ion is split in two in the ligand field: doubly-degenerated ^2E (e_g) and triply-degenerated $^2T_2$ (t_{2g}). Then, the two peaks a and b in the calculated absorption spectra (Fig. 5) are associated with the anti-bonding O2p^* states that are hybridized with the anti-bonding Hf 5d^*. The structure c corresponds to transitions to anti-bonding Hf 6s^* states. The splitting between a and b which is called 'effective crystal-field splitting' is found to be $\Delta(d*_{1,2}) = 4.28$ eV for $\mu(2°)$, $\Delta(d*_{1,2}) = 3,9$ eV for $\mu(4°)$ and $\Delta(d*_{1,2}) = 4.05$ eV for $\mu(5°)$. The splitting between a and c is found to be $\Delta(d*_1, s*) \approx 8.4$ eV in all spectra. The values obtained agree well with experimental values of $\Delta(d*_{1,2}) = 4.3$ eV and $\Delta(d*_1, s*) = 9.0$ eV for HfO$_2$ from Ref. [18,21].

According to Ref. [27,28] in crystalline ZrO$_2$ the separation as well as the depth of the minimum between the first two peaks reflects the specific polymorph (cubic, tetragonal or monoclinic). Similar trends are likely for HfO$_2$ polymorphs. Both oxides show phase transformations from monoclinic to tetragonal to cubic as the temperature increases. In the pure form both of cubic and tetragonal phases contain ZrO$_8$ polyhedra and are based on fluorite lattice. c-ZrO$_2$ is constructed from regular ZrO$_8$ polyhedra where the oxygen atoms are positioned in the corners of a cube with the Zr atom at the body center. t-ZrO$_2$ remains essentially cubic but there is some distortion in this phase. The e_g - t_{2g} splitting of the Zr d states will be retained, although some broadening might be expected. The monoclinic phase in ZrO$_2$ is described as a distorted fluorite structure with the Zr atoms in sevenfold coordination sites. Because m-ZrO$_2$ consists of ZrO$_7$ polyhedra the situation is more complicated. In this case a complex splitting of the d orbital is possible [27]. Finally this phase can be described as combination of ZrO$_8$ and ZrO$_7$ polyhedra. Calculations of the ZrO$_2$ polymorphs show that an increase in symmetry is associated with a greater peak splitting and narrower peaks [27,28].

Because of the amorphous structure of our HfO$_2$ film, we are not convinced that the shift of the structure in the absorption spectra versus the glancing angle comes from a transition from one phase of crystalline HfO$_2$ to another one. Nevertheless, we guess that the possible heterogeneity in the depth profile evidences a non-homogeneous character of the amorphous HfO$_2$ film. In Ref. [19,21] the variations of peak splitting and peak width are

connected with structural rearrangements (different oxygen coordination around the metal ions) and/or reduction in the point defect concentration.

The preceding discussion allows us to explain the changes with the depth in the calculated absorption spectra by the modification of the local environment of the oxygen atoms and/or the reduction in number of point defects, which could arise from oxygen vacancies. According to Fig. 5 only the spectrum $\mu(2°)$ is characterized by a low contrast and large broadening of the peaks *a* and *b*. All other spectra show similar sharp peaks *a* and *b*. Since it has been noted that the energy position of the *b* feature does not change for glancing angles from 4°, this suggests that there is only a thin surface layer with a disordered structure in the investigated sample. As stated above there is a rather good agreement of calculated spectra for glancing angles equal to or larger than 4° with EELS and XAS spectra from Ref. [19,17]. For example, $\mu(5°)$ is well correlated with the EELS spectrum from Ref. [19] (see Figure 6), which according to the authors shows the good structural quality of the sample.

IV. Conclusion

The x-ray reflection spectroscopy near the O-K absorption edge appears to be a non-destructive method convenient for the depth profiling of metallic oxides and particularly of "high-k" materials. This study has allowed us to show that our HfO_2 amorphous film has a well defined structure with a thin superficial layer presenting defect points or various local atomic structures.

References

[1] S. I. Association, The International Roadmap for Semiconductors (Sematech, Austin, TX, 2000), http://public.itrs.net/.

[2] G. D. Wilk, R. M. Wallace, and J. M. Anthony, J. Appl. Phys. **89**, 5243 (2001).

[3] A. I. Kingon, J.-P. Maria, and S. K. Streiffer, Nature **406**, 1032 (2000).

[4] C. T. Hsu, Y. K. Su, and M. Yokoyama, Jpn. J. Appl. Phys. **31**, 2501 (1992).

[5] K. Kukli, J. Arik, A.Aidla, H.Simon, M. Ritala, and M. Leskela, Appl. Surf. Sci. **112**, 236 (1997).

[6] M.-H. Cho, Y. S. Roh, C. N. Whang, K. Jeong, S. W. Narm, D.-H. Ko, J. H. Lee, and K. Fujihara, Appl. Phys. Lett. **81**, 472 (2002).

[7] J.-C. Lee, S.-J. Oh, M.Cho, C. S. Hwang, and R. Jung, Appl. Phys. Lett. **84**, 1305 (2004).

[8] P. Punchaipetch, T. Okamato, H. Nacamura, Y. Uraoka, T. Fuyuki, and S. Horii, Jpn. J. Appl. Phys. **43**, 7815 (2004).

[9] A. Ohta, H. Nacagawa, H. Murakami, S. Higashi, T. Kawahara, K. Torii, and S. Miyazaki, J. Appl. Phys. **43**, 7831 (2004).

[10] H. Nakagawa, A. Ohta, F. Takeno, S. Nagamachi, H. Murakami, S. Higashi, and S. Miyazaki, J. Appl. Phys. **43**, 7890 (2004).

[11] K. P. Bastos, C. Driemeier, R. P. Pezzi, G. V. Soares, L. Miotti, J. Moarais, I. J. R. Baumvol, and R. M. Wallace, Mat. Sci. Eng. B**112**, 134 (2004).

[12] C. S. Kang, H.-J. Cho, K. Onishi, R. Nieh, R. Choi, S. Gopalan, S. Krishman, J. H. Han, and J. C. Lee, Appl. Phys. Lett. **81**, 2593 (2002).

[13] J. Zhu, Y. R. Li, and Z. G. Liu, J. Phys. D: Appl. Phys. **37**, 2896 (2004).

[14] L. Xie, Y. Zhao, and M. H. White, Solid State Electronics **48**, 2071 (2004).

[15] V. Rangarajan, H. Bhandari, and T. M. Klein, Thin Solid Films **419**, 1 (2002).

[16] O. Renault, D. Samour, D. Rouchon, P. Holliger, A.-M. Papon, D. Blin, S. Marthon, Thin Solid Films **428**, 190 (2003).

[17] G. Lucovsky, Y. Zhang, G. B. Rayner Jr., G. Appel, and H. Ade, J. Vac. Sci. Technol. B**20**, 1739 (2002).

[18] G. Lucovsky, J. G. Hong, C. C. Fulton, Y. Zou, R. J. Nemanich, and H. Ade, J. Vac. Sci. Technol. B**22**, 2132 (2004).

[19] G. D. Wilk, and D. A. Muller, Appl. Phys. Lett. **83** 3984 (2003).

[20] J. G Chen, Surf. Sci. Rep. **30**, 1 (1997).

[21] S. Stemmer, Z. Q. Chen, W. J. Zhu, and T. P. Ma, J. Microsc. **210**, 74 (2003).

[22] E. O. Filatova, A. Stepanov, C. Blessing, J. Friedrich, R. Barchewitz, J-M André, F. Le Guen, S. Bac, and P. Troussel, J. Phys.: Condens. Matter **7**, 2731 (1995).

[23] E. O. Filatova, J-M. André, E. Yu. Taracheva, A. G. Tvaladze, V. L. Krazman, A. A. Novakovich, and R. V. Vedrinskii, J. Phys.: Condens. Matter **16**, 4597 (2004).

[24] B. L. Henke, P. Lee, T. J. Tanaka, R. I. Shimabukuro, and B. K. Fujikawa, At. Data Nucl. Data Tables **27**, 1 (1982).

[25] E. O. Filatova, V. A. Lukyanov, R. Barchewitz, J.-M. André, M. Idir, and P. Stemler, J. Phys.: Condens. Matter **11**, 3355 (1999).

[26] C. Weimer, S. Ferrari, M. Fanciulli, G. Pavia, and L. Lutterotti, Thin Solid Films **450**, 134 (2004).

[27] D. W. McComb, Phys. Rev. B**54**, 7094 (1996).

[28] S. Ostanin, E. Salamatov, A. E. Graven, D. W. McComb, and D. Vlachos, Phys. Rev. B**66**, 132105 (2002).

[16] P. Jonnard, I. Jarrige, O. Renault, J.-F. Damlencourt, and F. Martin, Surf. Sci. **572**, 396 (2004).

[17] V. R. Galakhov, E. Z. Kurmaev, S. N. Shamin, V. V. Fedorenko, L. V. Elokhina, J. C. Pivin, S.Zaima, and J. Kojima, Thin Solid Films **350**, 143 (1999).
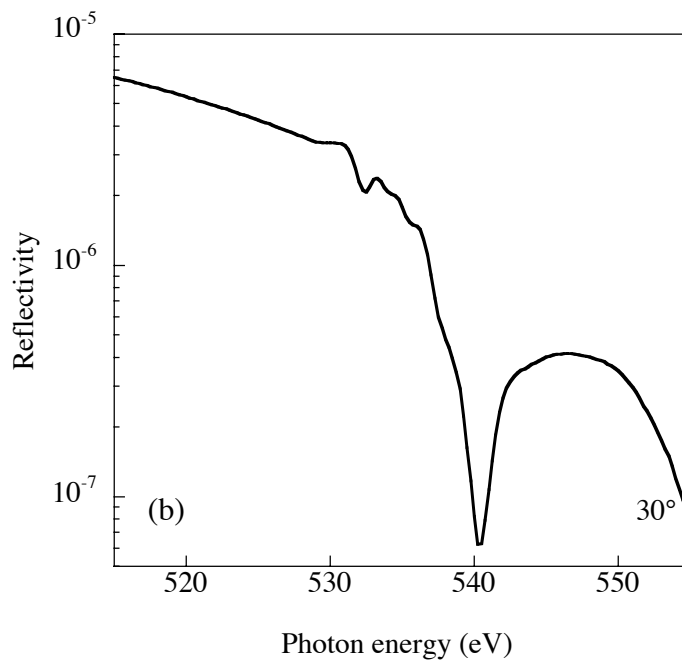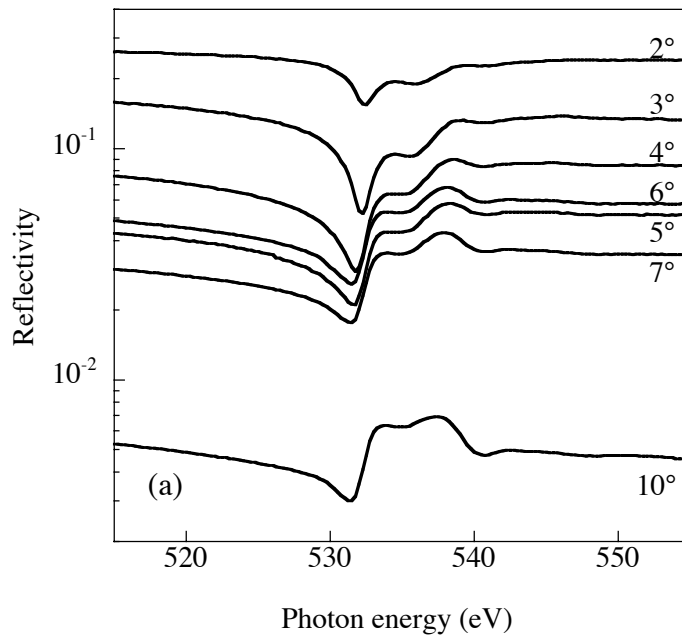
Table captions

Fig. 1: Reflection spectra of the $HfO_2/SiO_2/Si$ system for various glancing angles between 2 and 10° (a) and for 30° (b).
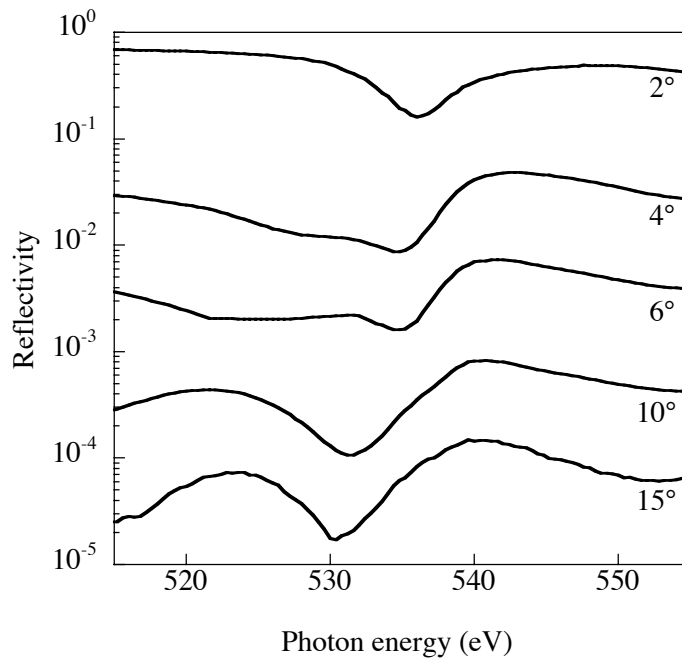
Fig. 2: Reflection spectra of the SiO_2/Si system for various glancing angles between 2° and 15°.

Fig. 3: Reflection coefficients calculated in the framework of the Fresnel approach for HfO_2 (thick line) and SiO_2 (thin line), at 520 eV (solid line) and at 540 eV (dashed line).

Fig. 4: Calculated angular dependency of the radiation penetration depth for different incident photon energies in HfO_2: 510 eV (solid line), 540 eV (dashed line) and 550 eV (dotted line).

Fig. 5 : Absorption spectra in the vicinity of the O-K edge in the $HfO_2/SiO_2/Si$ system calculated from the experimental reflection spectra by means of the Kramers-Kronig relations, for various glancing angles : 2° (solid line), 3° (dashed line), 4° (dotted line) and 5° (dashed-dotted line).

Fig 6 : Absorption spectra in the vicinity of the O-K edge in the $HfO_2/SiO_2/Si$ system calculated from the experimental reflection spectra for a 5° glancing angle (line) compared with the EELS spectrum of Ref. [19] (dots).

Fig. 1: Reflection spectra of the HfO$_2$/SiO$_2$/Si system for various glancing angles between 2 and 10° (a) and for 30° (b).

Fig. 2: Reflection spectra of the SiO$_2$/Si system for various glancing angles between 2° and 15°.
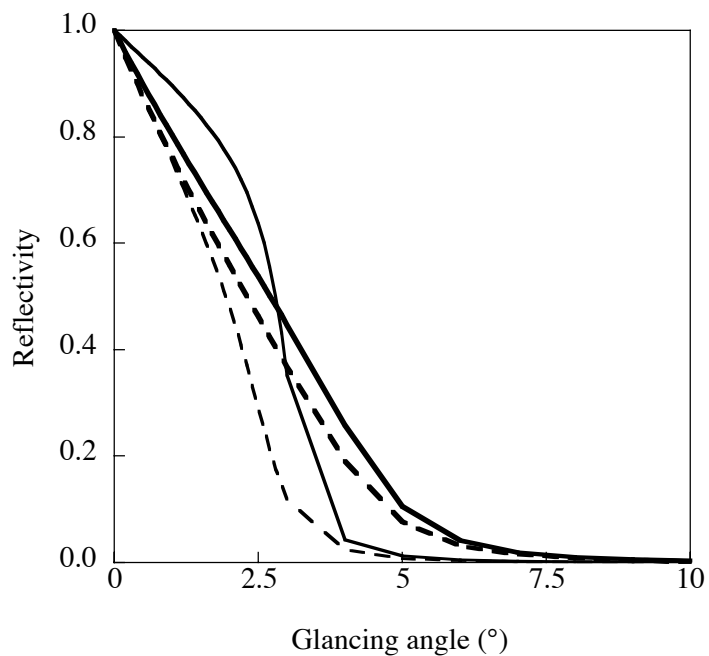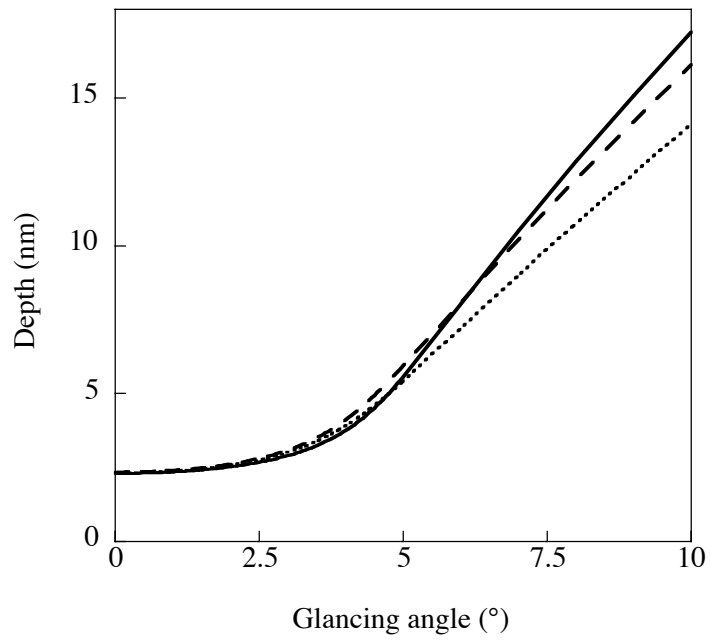
Fig. 3: Reflection coefficients calculated in the framework of the Fresnel approach for HfO$_2$ (thick line) and SiO$_2$ (thin line), at 520 eV (solid line) and at 540 eV (dashed line).

Fig. 4: Calculated angular dependency of the radiation penetration depth for different incident photon energies in HfO_2: 510 eV (solid line), 540 eV (dashed line) and 550 eV (dotted line).
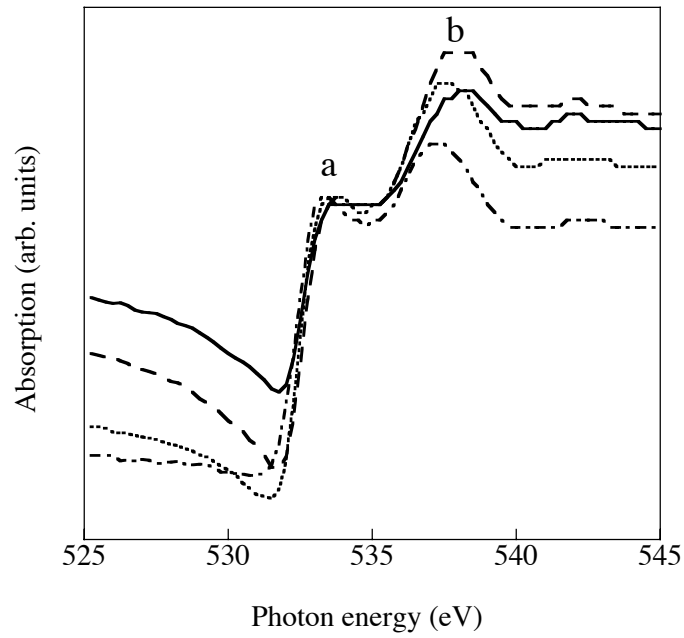
Fig. 5 : Absorption spectra in the vicinity of the O-K edge in the $HfO_2/SiO_2/Si$ system calculated from the experimental reflection spectra by means of the Kramers-Kronig relations, for various glancing angles : 2° (solid line), 3° (dashed line), 4° (dotted line) and 5° (dashed-dotted line).
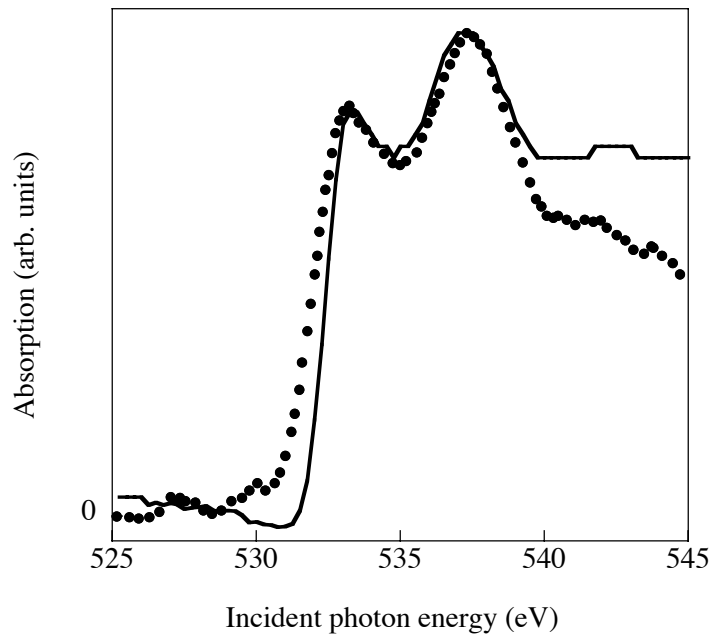
Fig 6 : Absorption spectra in the vicinity of the O-K edge in the $HfO_2/SiO_2/Si$ system calculated from the experimental reflection spectra for a 5° glancing angle (line) compared with the EELS spectrum of Ref. [19] (dots).